nature geoscience

Supplementary information https://doi.org/10.1038/s41561-024-01559-2

Direct and lagged climate change effects intensified the 2022 European drought

In the format provided by the authors and unedited

Contents

1 The extremeness of the 2022 summer soil moisture droughts in CLM–ERA5 simulations

To further inspect the soil moisture drought, we also considered the CLM–ERA5 model setup. Even though this model setup is far more complex than mHM–E-OBS, the latter outperforms it (compare Supplementary Figure 6 and Extended Data Figure 1), for example, in the simulation of the spatial pattern of the 2022 total water storage anomaly (panels g,h). Still, we note that, compared to mHM–EOBS and observations, CLM–ERA5 ranks the 2022 drought as the third, rather than first, driest year since 2002 in terms of June–August total water storage (Supplementary Figure 6d), and as the second driest in terms of soil moisture (Supplementary Figure 5). Such a discordance arises from the ranking of the last 20-year summers (compare Figure 1 and Supplementary Figure 5), a period in which CLM–ERA5 does not align well with the ranking in satellite observations. Note that this also affects the spatial extent of the drought, which is more contained in CLM–ERA5 simulations (Supplementary Figure 5c). Therefore, it is well possible that the 2022 drought extremeness is not well represented in CLM–ERA5 and that 2022 was not only one of the most extreme since 1960, but the most extreme. The discordance of CLM–ERA5 might stem from the forcing ERA5 data, given that mHM performances decrease when it is forced by ERA5 (compare Extended Data Figure 1 and Supplementary Figure 7). In particular, ERA5 overestimates mean precipitation and wet days[1] and shows much less strong negative trends in precipitation over the recent years compared to E-OBS (Supplementary Figure 8). These differences are more pronounced than for temperature, and we note that among various other in-situ or remotely sensed measurements, ERA5 assimilates 2m-temperature — but not precipitation — from Surface Synoptic Report (SYNOP) information collected by weather stations operated by National Meteorological Services around the globe[2]. We thus consider ERA5 precipitation trends in a region with a comparatively dense observational network such as Europe less reliable compared to purely observational datasets such as E-OBS[1]. Furthermore, the misrepresentation of the total water storage extremeness in 2022 persists when employing mHM–ERA5 (Supplementary Figure 7b-d; see circled dot in the bottom-left corner), which further indicates that E-OBS is more suitable than ERA5 for forcing the simulations.

2 Supplemental Methods

Data and Historical land surface model simulations (CLM–ERA5)

To provide an additional line of evidence, in addition to the hydrological simulations based on mHM, we also used the Community Land Model (CLM)[3,4] to simulate soil moisture. CLM is a more complex model than mHM as it simulates not only hydrological processes but also energy and carbon fluxes, and it serves as the land component of the fully coupled Community Earth System Model (CESM), such that the physical, chemical, and biological processes underlying interactions between climate and terrestrial ecosystems can be examined. To evaluate the model (Supplementary Figure 6), we also simulated total water storage anomaly and followed the same procedure employed for mHM. CLM simulations were performed in offline mode with 3-hourly meteorological forcing from ERA5 reanalyses (across the global landmasses)[2], consisting of precipitation, temperature, specific humidity, downwelling shortwave radiation, wind speed and surface pressure. CLM was compiled in data atmosphere (DATM) mode for version 4.5 using satellite phenology, with the forcing obtained from ERA5 at a horizontal resolution of 0.5°. Using this configuration, a baseline simulation was performed from 1956 onwards, although values prior to 1960 are not considered for analysis to allow for soil moisture model spin-up. The soil moisture computed by CLM at a horizontal resolution of 1.25° x 0.9° was aggregated to a depth of 2.0m, weighting the lowermost soil layer by a fraction to take into account that it extends further down than the required target depth. To allow for a robust comparison of the CLM and mHM simulations, we considered CLM output over the same domain considered for mHM-based analyses.

The representation of evaporation is important for drought and may influence uncertainties in the impact of climate variability and change on the European drought. Therefore, here we discuss how CLM compares to other models. Given available moisture in the soil, supplied by precipitation, temperature affects the sensitivity of evaporation in the CLM model. Older intercomparison studies, including, among other models, the predecessor of the CLM version in an atmospheric general circulation model setup, indicate that the model simulates a coupling of soil moisture and temperature that is in line with the multi-model mean estimate[5]. This is relevant because the sensitivity of evaporation to both soil moisture and temperature plays an important role in this coupling. CLM is considered to be a state-of-the-art land surface model at the forefront of model development, and is frequently used for hydroclimatic analyses and more (often also as a component of entire Earth System Models[6]; note that CLM is not only the land model of the Community Earth System Model, but also of other Earth System Models such as NorESM). CLM has been shown to adequately capture the evolution of land surface energy and carbon fluxes as well as hydrological variables in evaluation studies, both at regional scales and when comparing to individual sites[7–10]. Although carbon fluxes are not directly relevant to our analysis, a realistic depiction of the terrestrial carbon sink mandates an adequate simulation of agro-ecological drought conditions, hence the use of a well-established and highly complex land surface model such as CLM – that portrays skill in simulating not just energy and water, but also carbon fluxes – makes our primarily mHM-based analysis more robust. Finally, we note that despite the good performance of the model, the performance of land surface models can depend on the parameter calibration[7], and that land surface models tend to share a number of general limitations, such as an overreliance on shallow soil moisture for evaporation[11], too conservative and idealized evaporation under soil drought conditions[12], lack of groundwater lateral flow and poor groundwater representation[13,14], and unrealistic stomatal conductance response to drought[15].

Counterfactual experiments to quantify the contribution of meteorological drivers and human-induced climate change (CLM–ERA5)

The climate input variables precipitation, temperature, specific humidity, and shortwave radiation were set to their respective climatologies to infer the meteorological drivers of the drought. We removed CMIP6 model trends from climate input variables to estimate the influence of climate change and lagged effect of climate change. This is analogous to our approach employed in mHM experiments to adjust precipitation, mean temperature, and daily temperature range. We refrained from modifying wind speed and surface pressure in all CLM experiments to simplify the comparison with mHM simulations. (Concerning humidity, since we adjusted only temperature, only specific humidity, or both in the relevant experiments, relative humidity changes are always implicit rather than assumed.) To allow for a comparison with mHM experiments for which we assessed the overall temperature contribution via assessing the combined contribution of anomalies of average temperature and daily temperature range (i.e. the contributions of all considered variables in mHM, except for precipitation), for CLM we assessed the contribution of temperature-related variables via also conducting simulations with all variables changed except for precipitation. Note that, because specific humidity and shortwave radiation are positively defined, we employed multiplicative (rather than additive) factors for these variables, as done for precipitation and daily temperature range for mHM.

To assess the climate change contribution, for the counterfactual experiments, we used the same CMIP6 climate model runs used for mHM simulations. In contrast to mHM counterfactual experiments for climate change for which the multiplicative and additive factors are derived from single CMIP6 models, for CLM we employed the multimodel mean of the factors and ran a unique simulation without assessing uncertainties due to climate model differences. This was required due to the much higher computational costs of running CLM compared to mHM. We note that the results of mHM based on the multimodel mean of the multiplicative/additive factors and the mean of the results based on the multiplicative/additive factors from individual climate models are similar (not shown), therefore enabling a coherent comparison of the CLM and mHM climate change contribution as presented in the manuscript.

Historical simulations via the mHM–ERA5 setup

To compare the performance of the mHM model forced with E-OBS data (mHM–E-OBS setup) with the performance of the model forced with ERA5 reanalysis (mHM–ERA5 setup), we additionally ran mHM historical simulations as described in the Method of the main text but forced with ERA5 reanalysis. Overall, this and the other simulations allow for comparing the performances of three setups (i.e., mHM–E-OBS, mHM–ERA5, and CLM-ERA5) in terms of total water storage anomalies against GRACE satellite observations.

3 Supplemental Figures

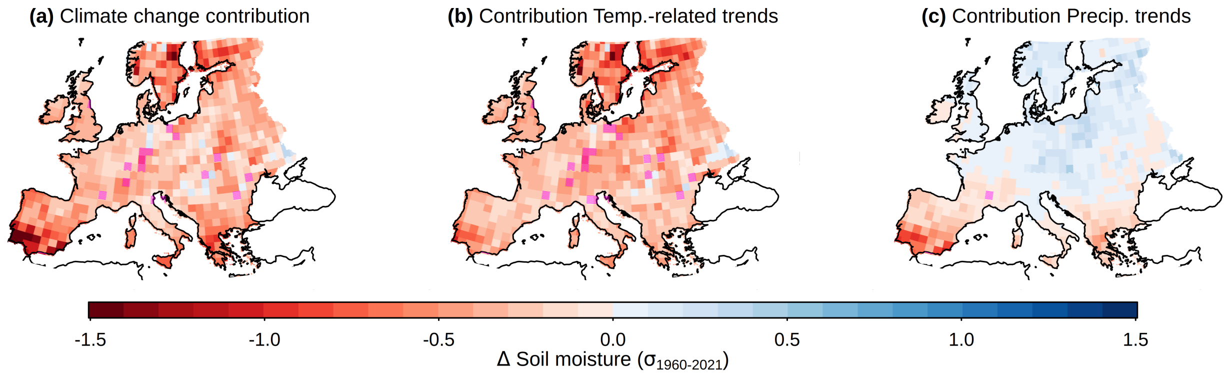

Supplementary Fig. 1. Contribution of human-induced climate change to the June–August 2022 soil moisture drought based on the CLM–ERA5 setup. The same as Figure 5, but based on the CLM–ERA5 setup. Note, we removed CMIP6 model trends both from temperature-related variables (i.e. temperature, radiation, and specific humidity) and precipitation in (a) and only from temperature-related variables in (b).

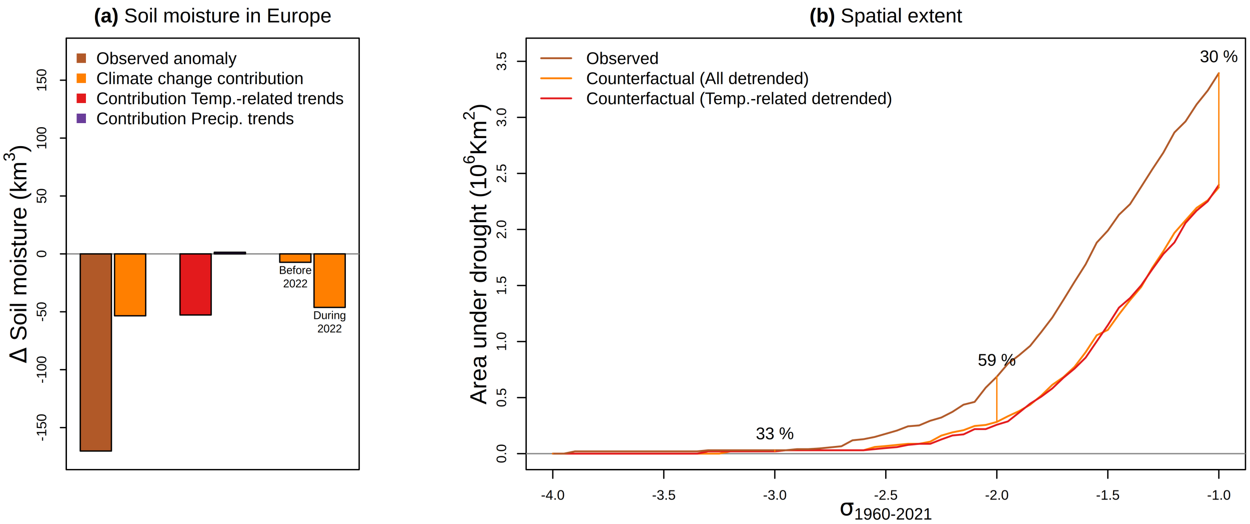

Supplementary Fig. 2. Effect of human-induced climate change to the European 2022 summer soil moisture drought. The same as Figure 6, but based on the CLM–ERA5 setup. Note that in (a) the "climate change contribution" and in (b) "All detrended" refers to the experiment within which we removed CMIP6 model trends both from temperature-related variables (i.e. temperature, radiation, and specific humidity) and precipitation. In panel b, the smaller climate change contribution to the area under drought in CLM–ERA5 compared to mHM–E-OBS (Figure 6) for most extreme droughts is in line with less extreme conditions simulated for 2022 by CLM–ERA5 compared to mHM–E-OBS.

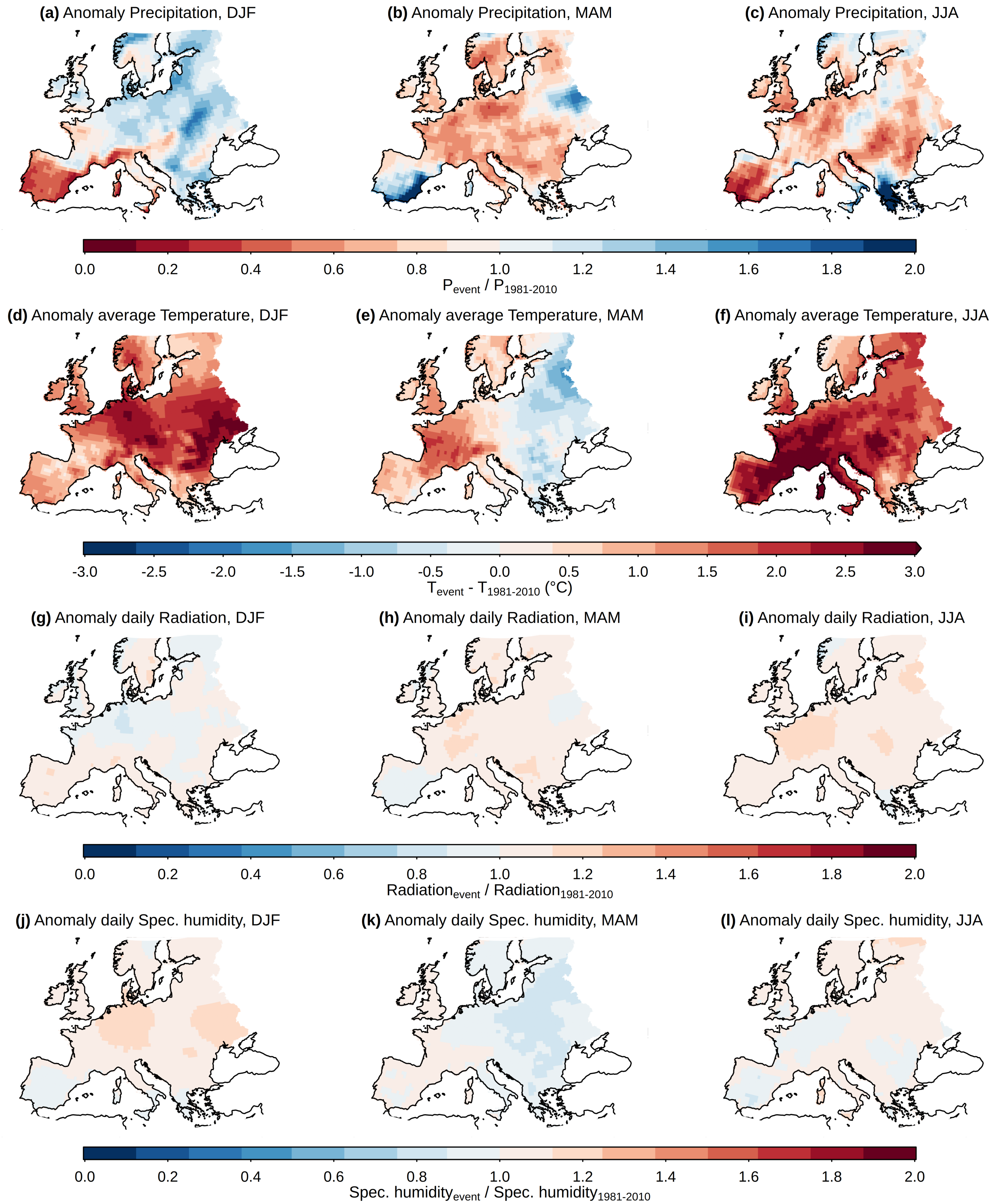

Supplementary Fig. 3. Seasonal weather anomalies before and during the summer drought based on ERA5 reanalyses. The same as Figure 2, but for ERA5 precipitation, temperature, downwelling shortwave radiation, and specific humidity.

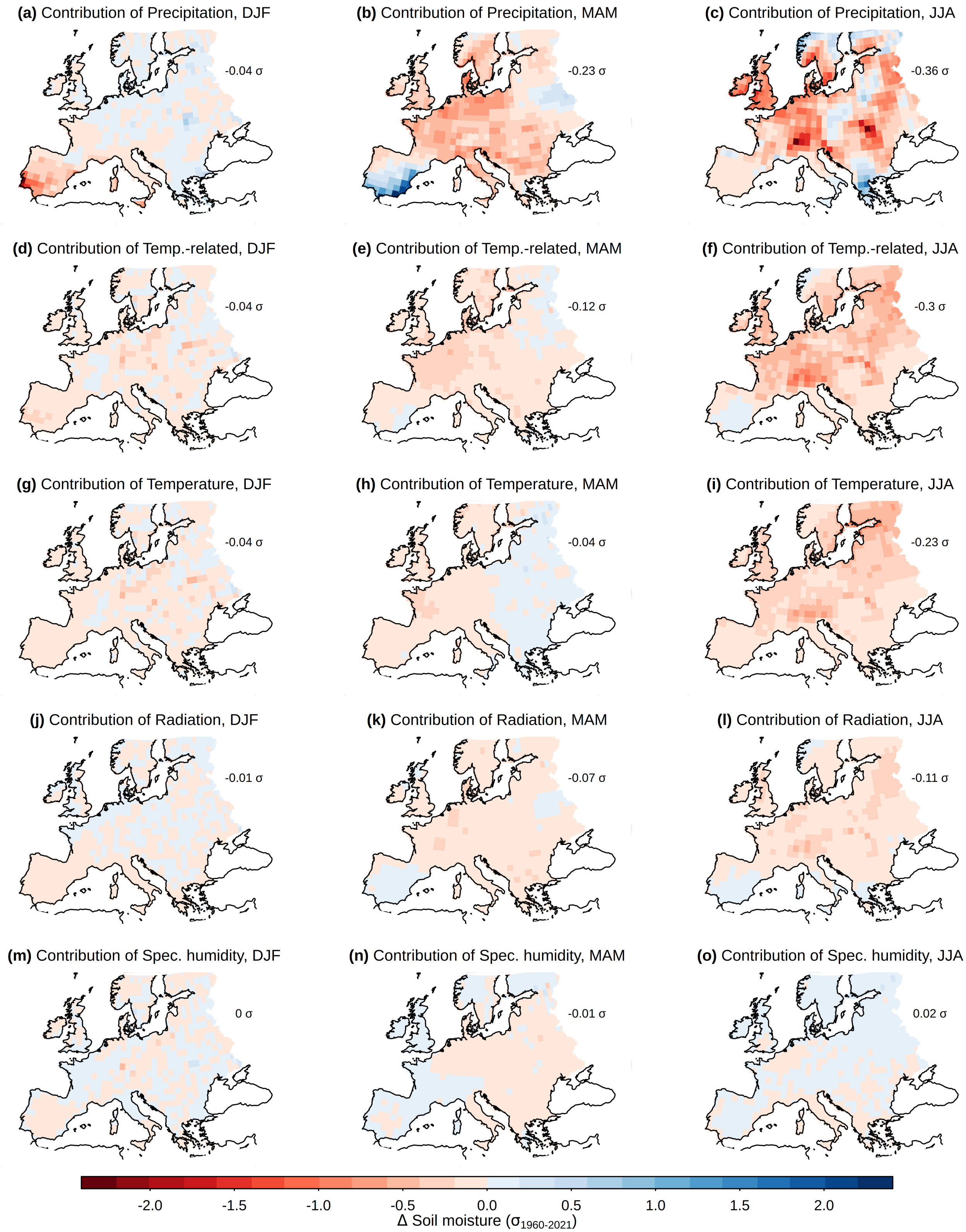

Supplementary Fig. 4. Contribution of weather anomalies to the June–August 2022 soil moisture drought based on the CLM–ERA5 setup. a-f, The same as Figure 3, but based on the CLM–ERA5 setup. Note that (d-f) shows the contribution from anomalies in temperature-related variables, which refers to the combined contribution of anomalies in temperature, radiation, and specific humidity (see Methods). **g-o**, The individual contributions of anomalies in (g-i) temperature, (j-l) downwelling shortwave radiation, and (m-o) specific humidity.

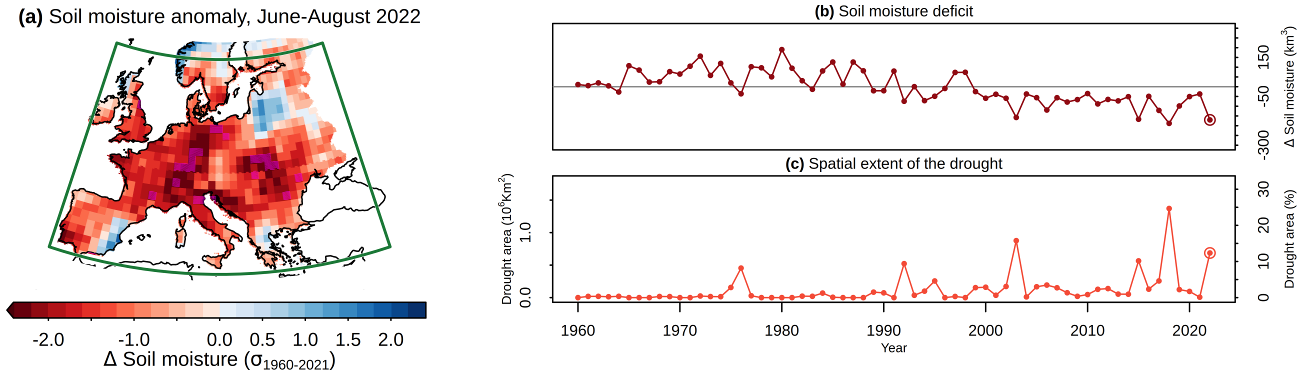

Supplementary Fig. 5. The 2022 European soil moisture drought based on the CLM–ERA5 setup. The same as Figure 1, but based on the CLM–ERA5 setup.

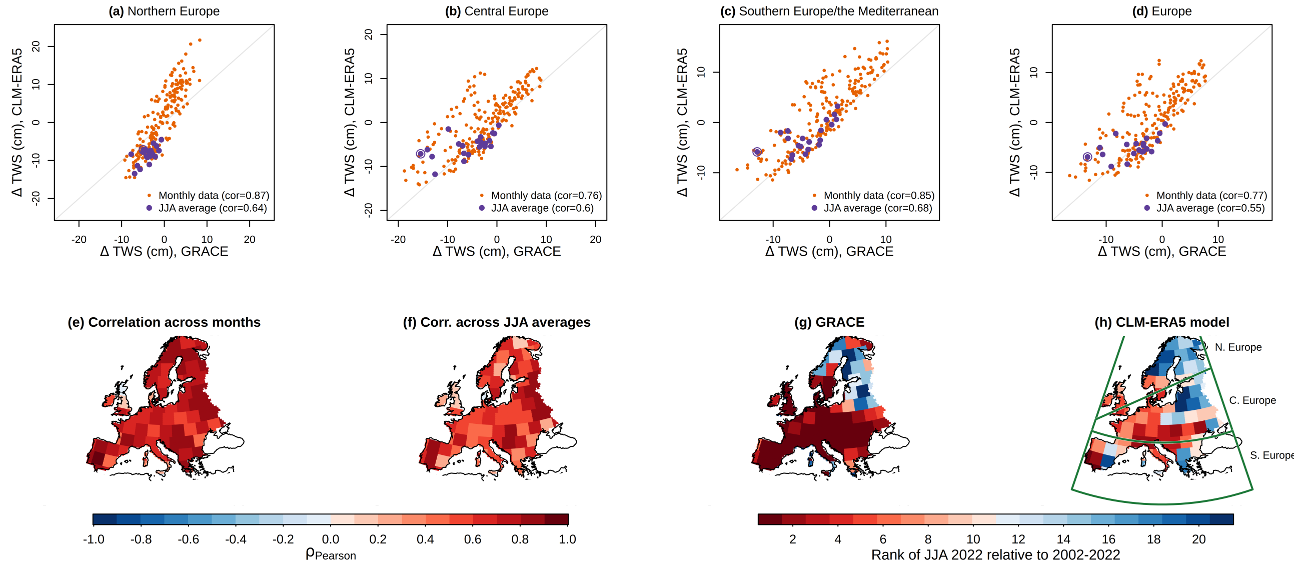

Supplementary Fig. 6. Evaluation of the CLM–ERA5 setup. The same as Extended Data Figure 1, but based on the CLM–ERA5 setup.

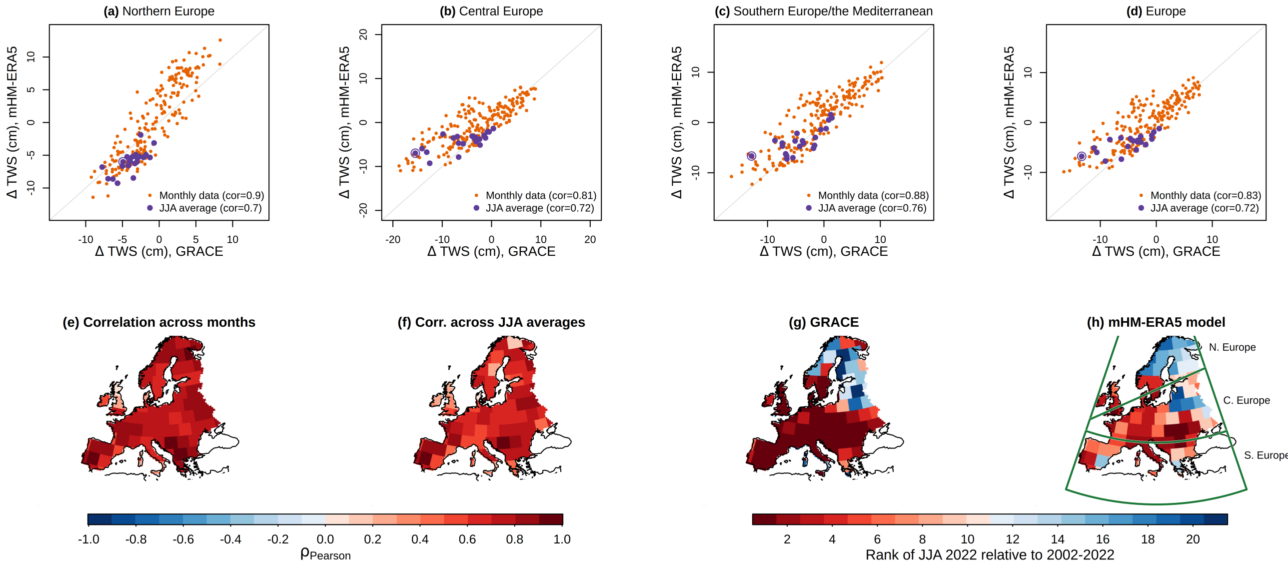

Supplementary Fig. 7. Evaluation of the mHM–ERA5 setup. The same as Extended Data Figure 1, but based on the mHM–ERA5 setup.

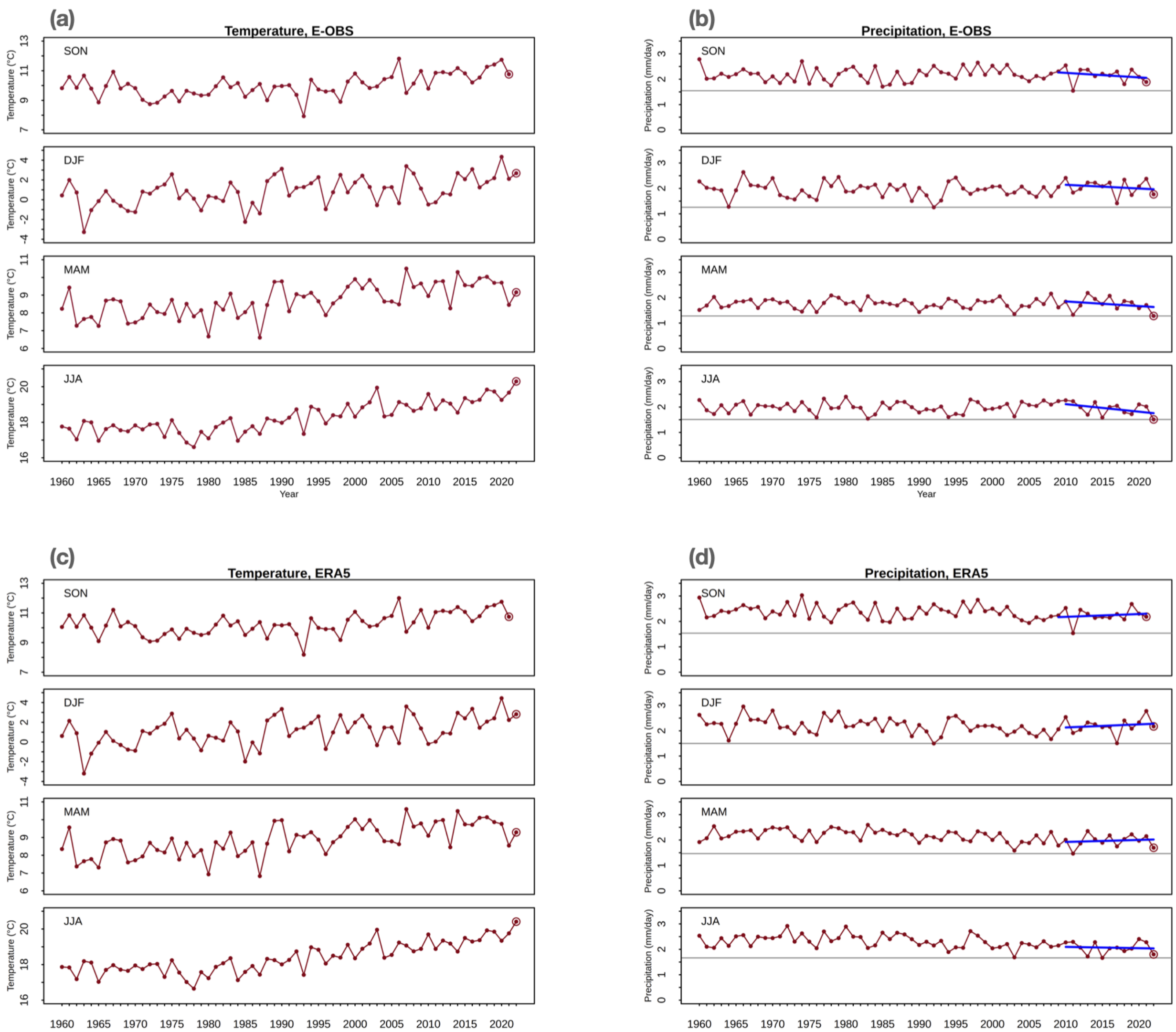

Supplementary Fig. 8. Time series of seasonal precipitation and temperature based on E-OBS and ERA5. a, Temperature time series averaged over Europe (box in Figure 1a) for September–November (SON), December–February (DJF), March–May (MAM), and June–August (JJA) based on E-OBS (period, from 1960 to SON 2022). **b**, The same as panel a, but for precipitation. The grey horizontal line shows the value of the driest observed season. The blue line shows the linear trend fitted to data starting in 2010 (starting in 2009 for SON). **c-d**, The same as panels a-b, but for data from ERA5.

References

1. Bandhauer, M. *et al.* Evaluation of daily precipitation analyses in E-OBS (v19. 0e) and ERA5 by comparison to regional high-resolution datasets in European regions. *Int. J. Climatol.* **42**, 727–747 (2022).
2. Hersbach, H. *et al.* The ERA5 global reanalysis. *Q. J. Royal Meteorol. Soc.* **146**, 1999–2049 (2020).
3. Lawrence, P. J. *et al.* Simulating the biogeochemical and biogeophysical impacts of transient land cover change and wood harvest in the Community Climate System Model (CCSM4) from 1850 to 2100. *J. Clim.* **25**, 3071–3095 (2012).
4. Oleson, K. W. & Lawrence, D. M. Technical Description of version 4.5 of the Community Land Model (CLM). NCAR Technical Note. Retrieved from URL: http://www.cesm.ucar.edu/models/cesm1.2/clm/CLM45_Tech_Note.pdf.
5. Koster, R. D. *et al.* GLACE: the global land–atmosphere coupling experiment. Part I: overview. *J. Hydrometeorol.* **7**, 590–610 (2006).
6. Hsu, H. & Dirmeyer, P. A. Soil moisture-evaporation coupling shifts into new gears under increasing CO2. *Nat. Commun.* **14**, 1162 (2023).
7. Duarte, H. F. *et al.* Evaluating the Community Land Model (CLM4. 5) at a coniferous forest site in northwestern United States using flux and carbon-isotope measurements. *Biogeosciences* **14**, 4315–4340 (2017).
8. Post, H. *et al.* Evaluation and uncertainty analysis of regional-scale CLM4. 5 net carbon flux estimates. *Biogeosciences* **15**, 187–208 (2018).
9. Cheng, Y. *et al.* Validation of the community land model version 5 over the contiguous United States (CONUS) using in situ and remote sensing data sets. *J. Geophys. Res. Atmospheres* **126**, e2020JD033539 (2021).
10. Ding, X., Lai, X. & Fan, G. Numerical simulation and evaluation of soil temperature on the Qinghai–Xizang Plateau by the CLM4. 5 model. *Theor. Appl. Climatol.* **152**, 371–384 (2023).
11. Dong, J., Lei, F. & Crow, W. T. Land transpiration-evaporation partitioning errors responsible for modeled summertime warm bias in the central United States. *Nat. Commun.* **13**, 336 (2022).
12. Li, W. *et al.* Contrasting drought propagation into the terrestrial water cycle between dry and wet regions. *Earth's Futur.* **11**, e2022EF003441 (2023).
13. Keune, J. *et al.* Studying the influence of groundwater representations on land surface-atmosphere feedbacks during the European heat wave in 2003. *J. Geophys. Res. Atmospheres* **121**, 13–301 (2016).
14. Felfelani, F., Lawrence, D. M. & Pokhrel, Y. Representing intercell lateral groundwater flow and aquifer pumping in the community land model. *Water Resour. Res.* **57**, e2020WR027531 (2021).
15. Green, J., Zhang, Y., Luo, X. & Keenan, T. Systematic underestimation of canopy conductance sensitivity to drought by Earth System Models. *AGU Adv.* **5**, e2023AV001026 (2024).